Electronic Supplementary Material (ESI) for Analytical Methods.


*Supplementary data*

# A turn-on fluorescent probe for $Lu^{3+}$ Recognition and Bio-Imaging in live cells and zebrafish

Mujthaba Aatif A[a], Selva Kumar R[a], S.K. Ashok Kumar[a]* and Abdul Majeed[b]

[a]Department of Chemistry, School of Advanced Sciences, Vellore Institute of Technology, Vellore-632014. Tamil Nadu, India. E-mail: ashokkumar.sk@vit.ac.in

[b]Department of Zoology and Aquatic Animal Health Laboratory, C. Abdul Hakeem College Melvisharam-632509, Tamil Nadu, India.

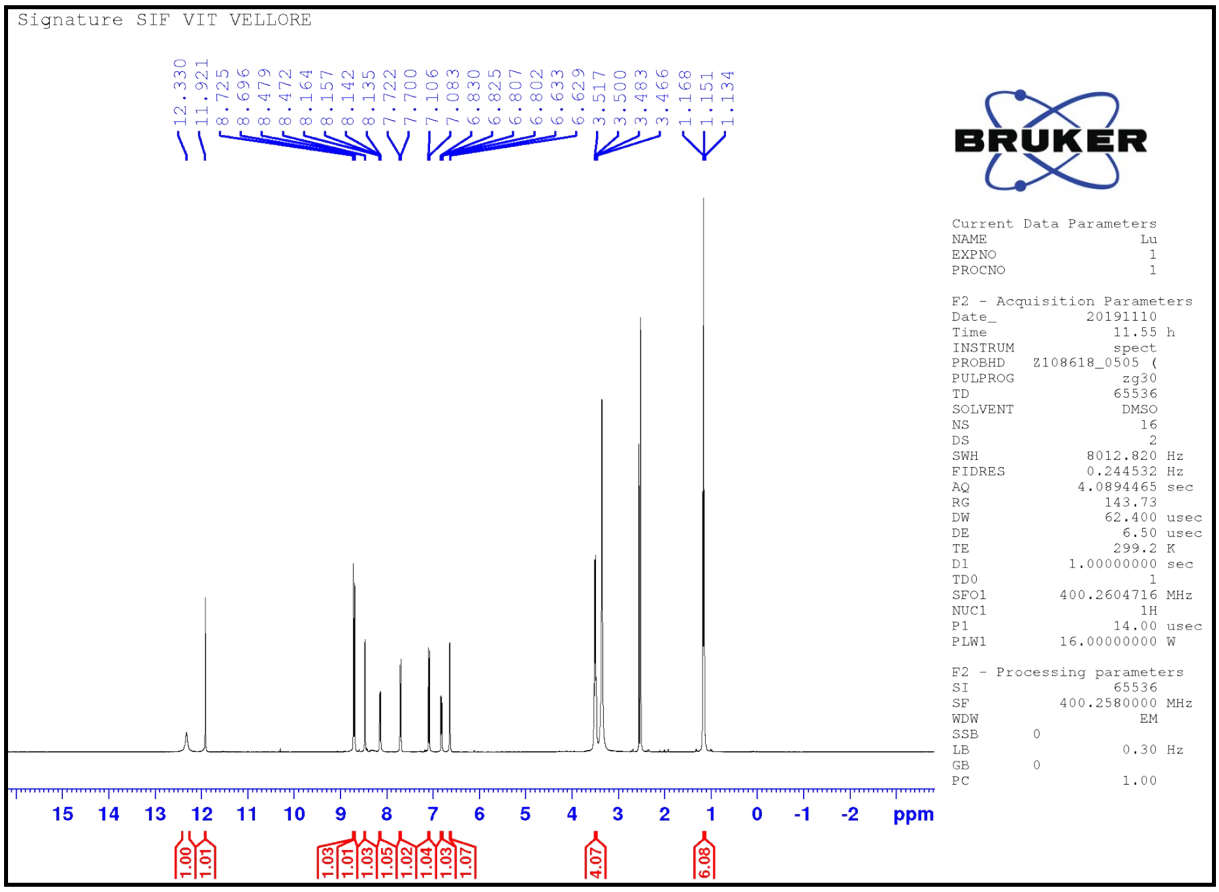


**Fig. 1S**. $^1$H NMR spectrum of **L**

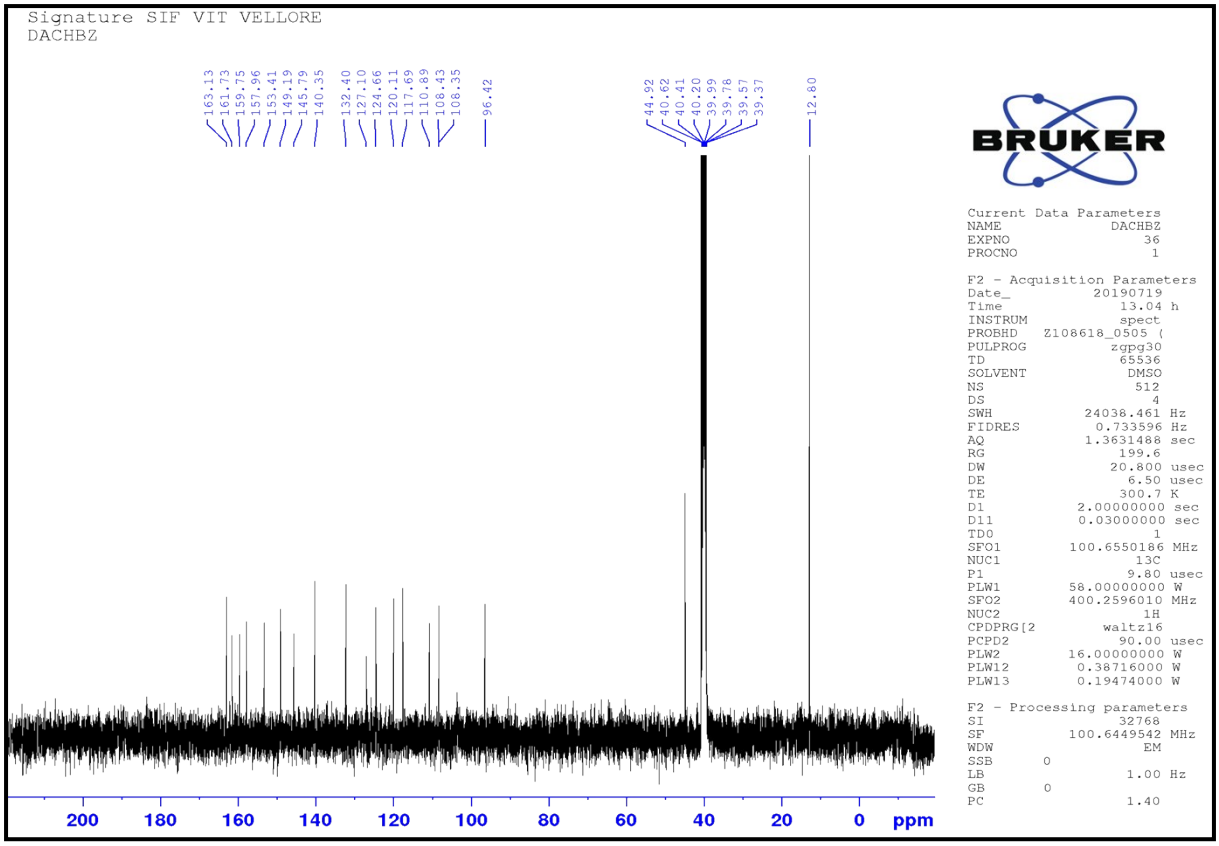


**Fig. 2S**. $^{13}C$ spectrum of **L**

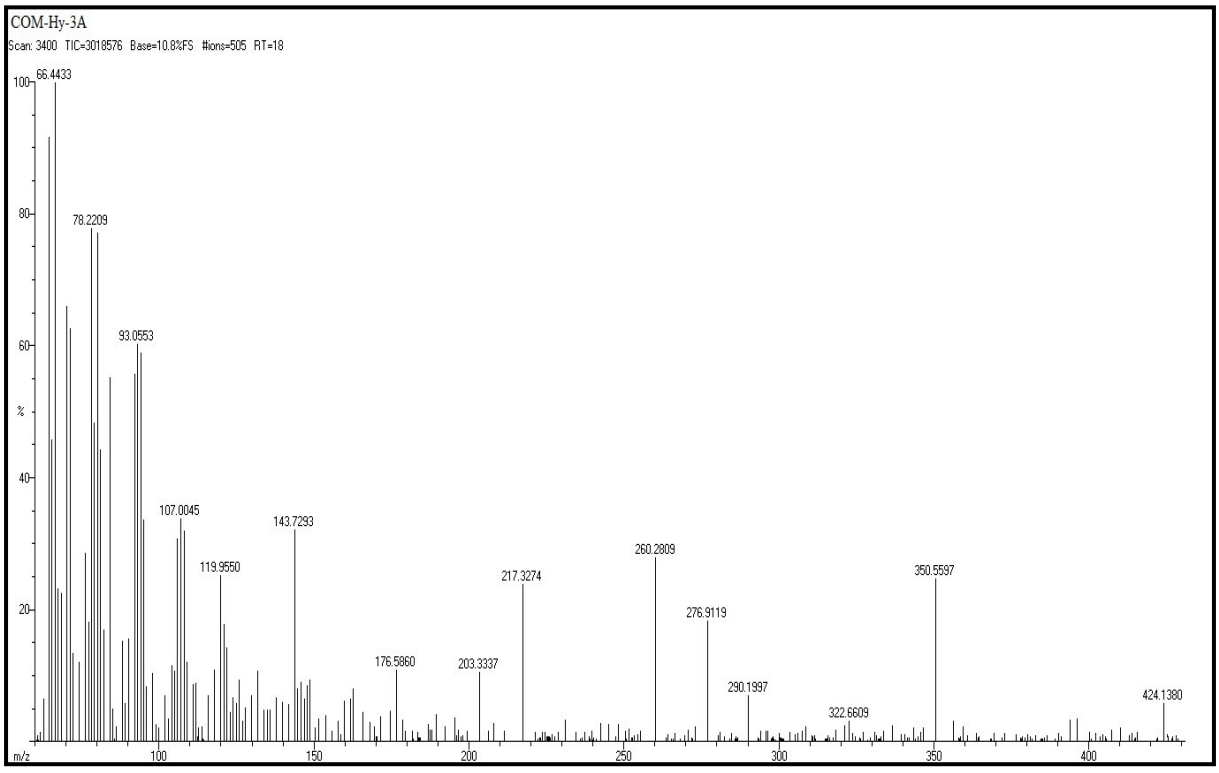


**Fig. 3S**. HR-Mass spectrum of **L**

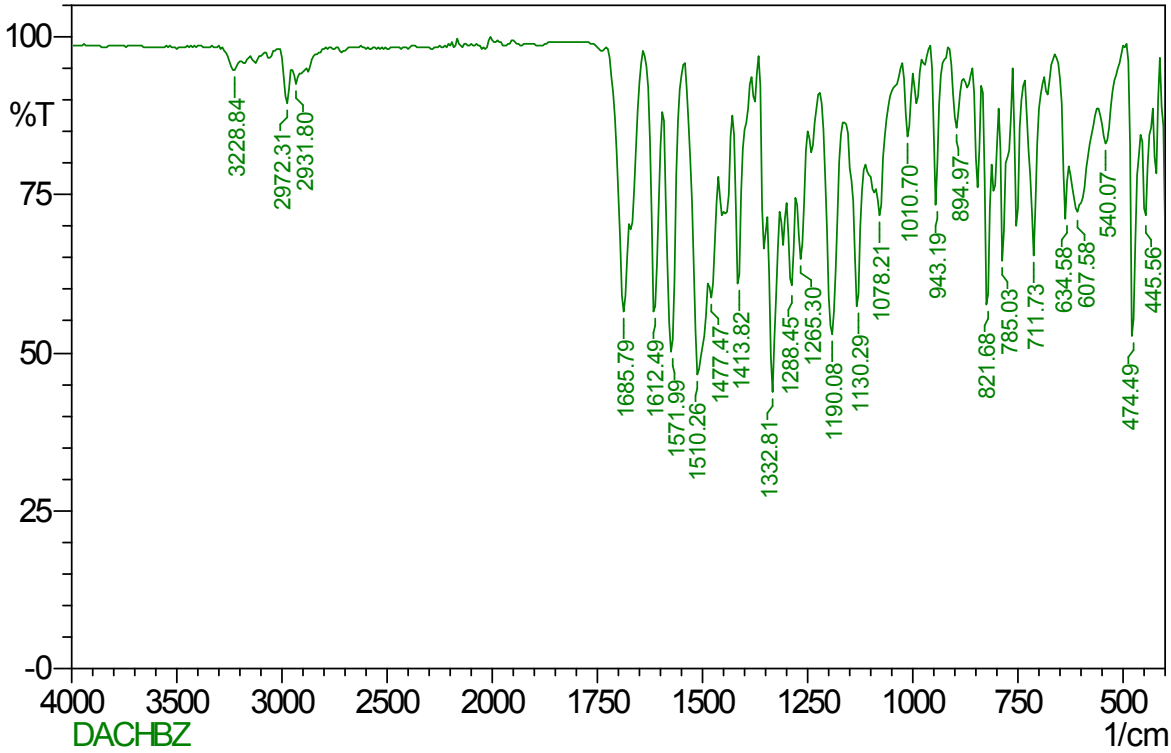


**Fig. 4S**. FTIR spectrum of **L**

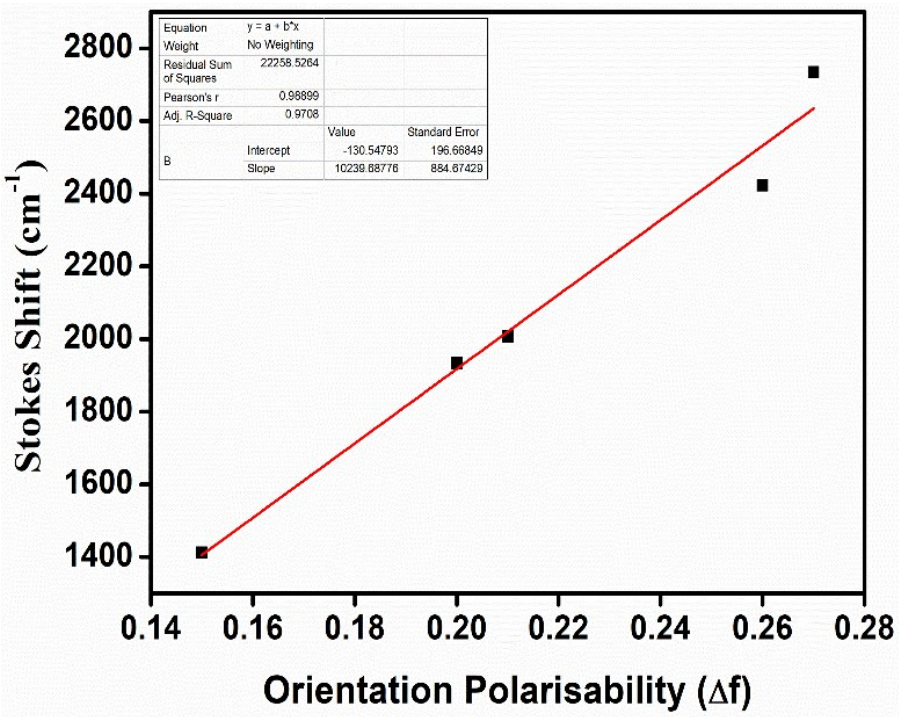


**Fig. 5S.** LM plot of **L**

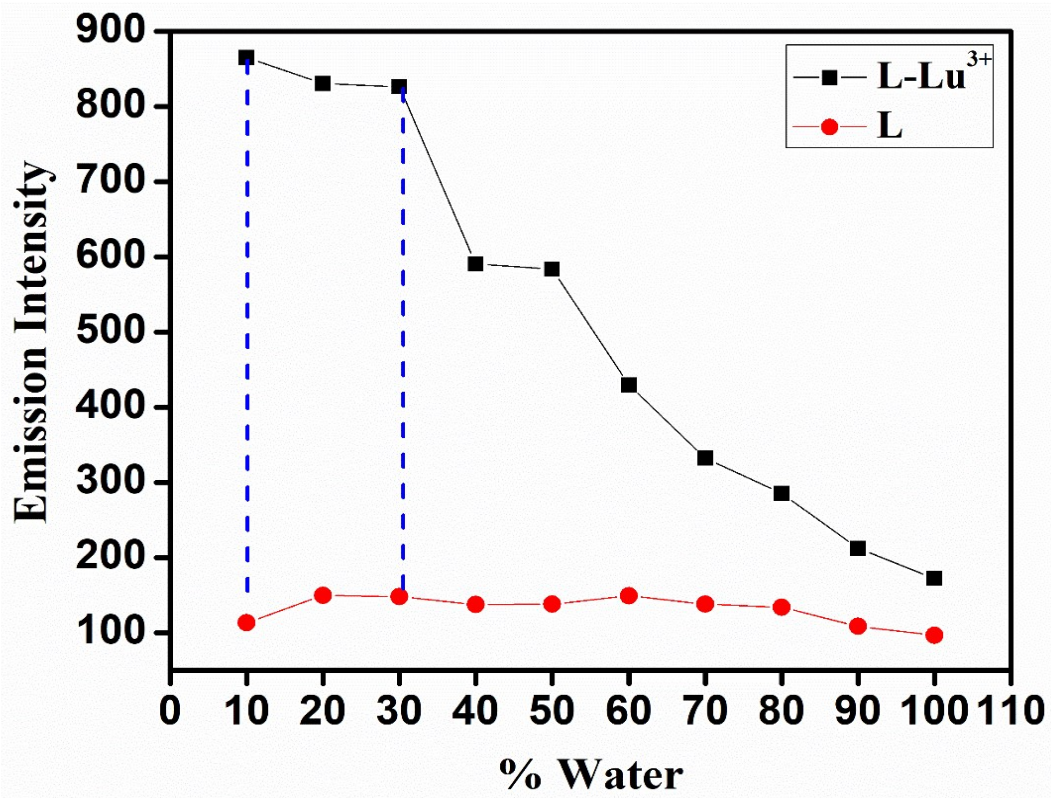


**Fig. 6S**. Effect of water content on **L** and **L-Lu**$^{3+}$

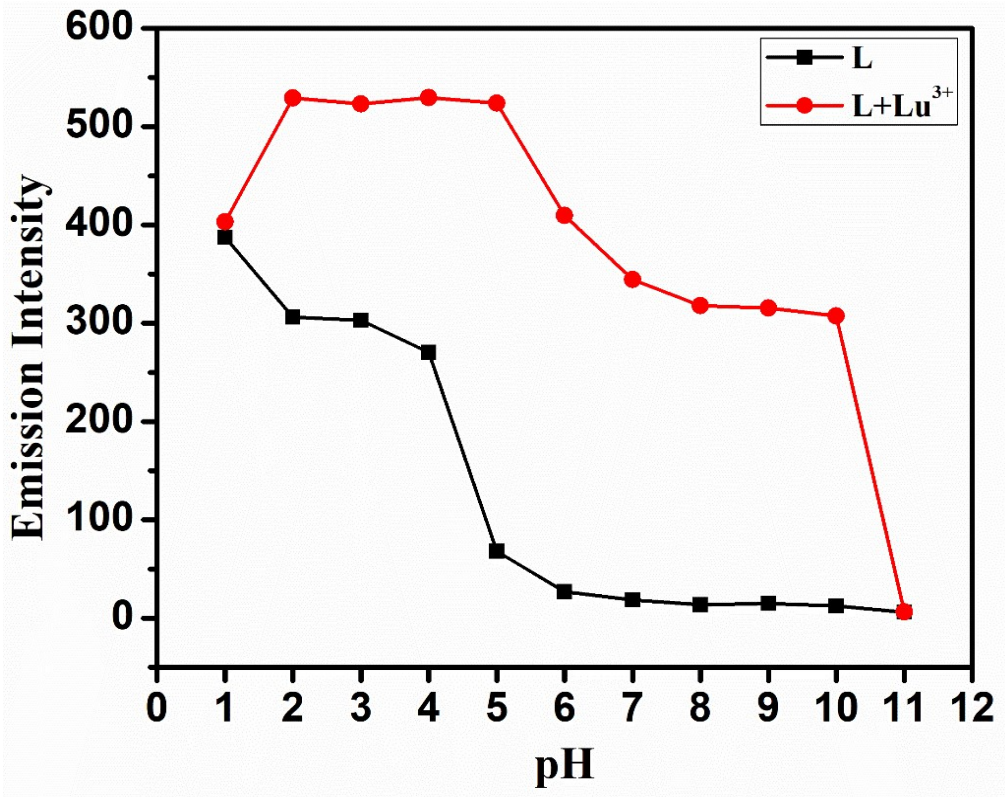


**Fig. 7S**. Effect of pH on **L** and **L-Lu**$^{3+}$

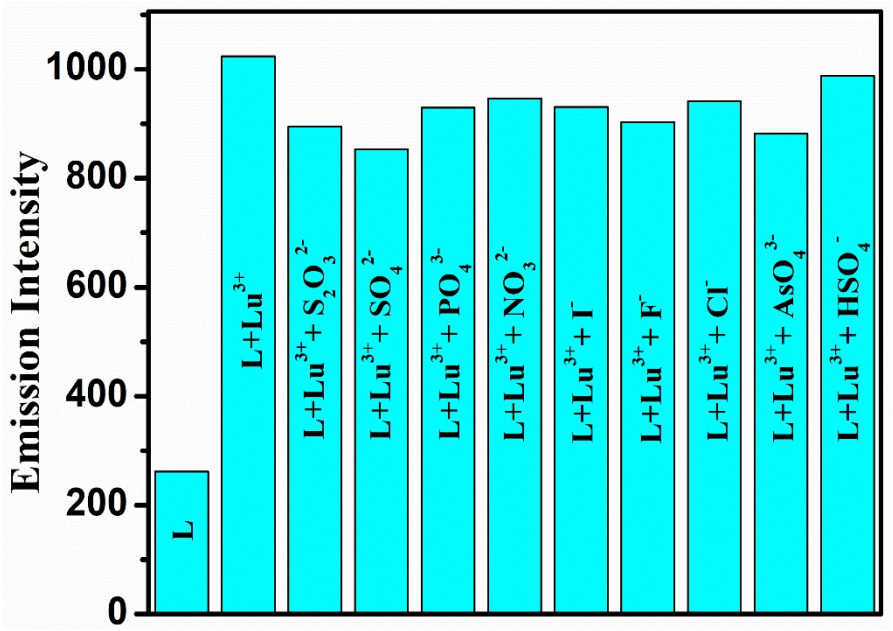


**Fig. 8S**. Effect of interfering anions on the performance **L** towards $Lu^{3+}$ determination

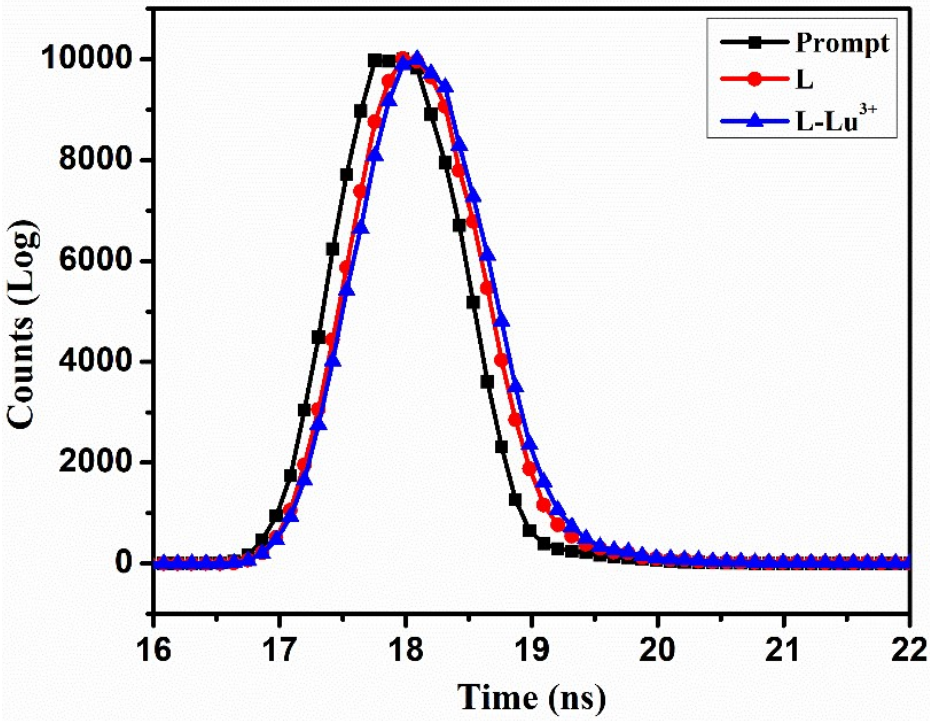


**Fig. 9S**. Time-resolved fluorescence decay analysis of **L** and **L-Lu$^{3+}$**.

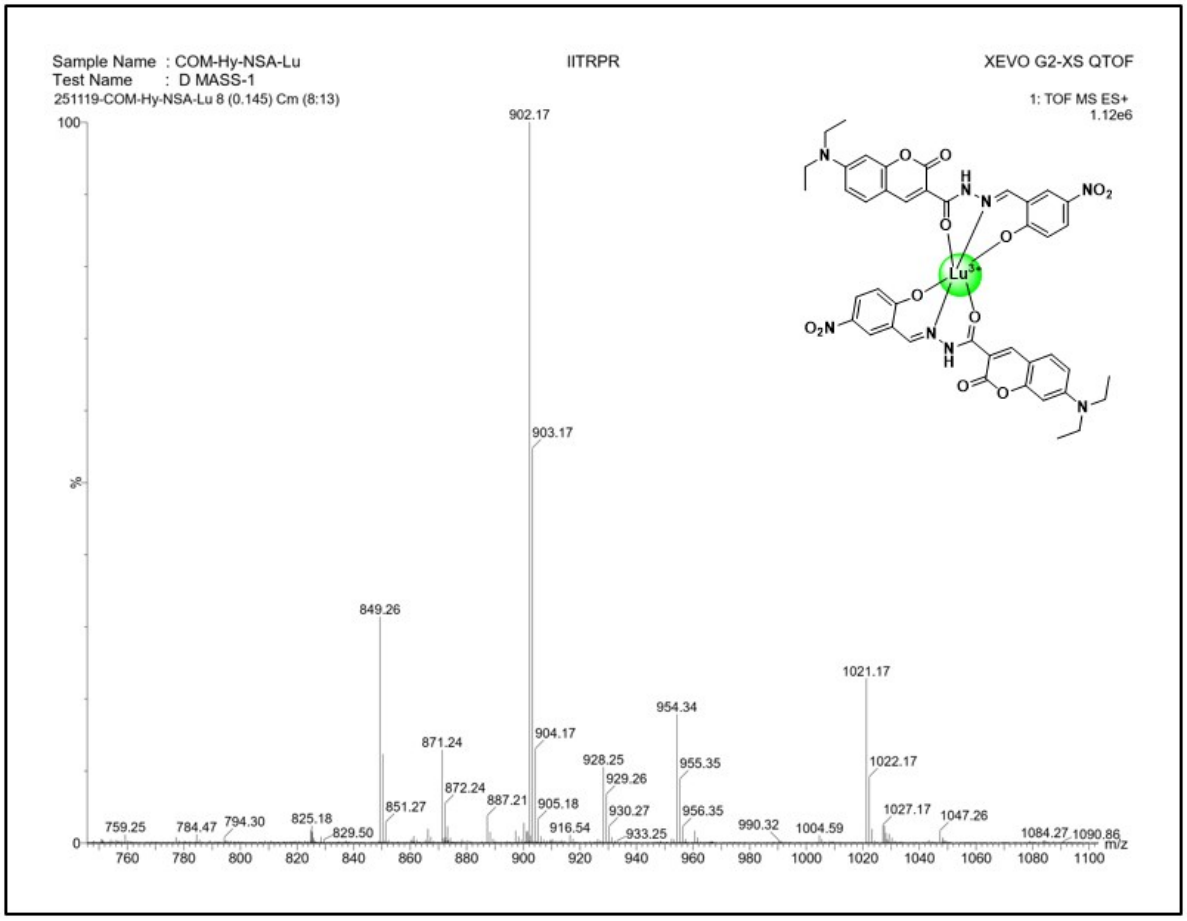


**Fig. 10S**. ESI-TOF mass spectrum of **L-Lu$^{3+}$** complex

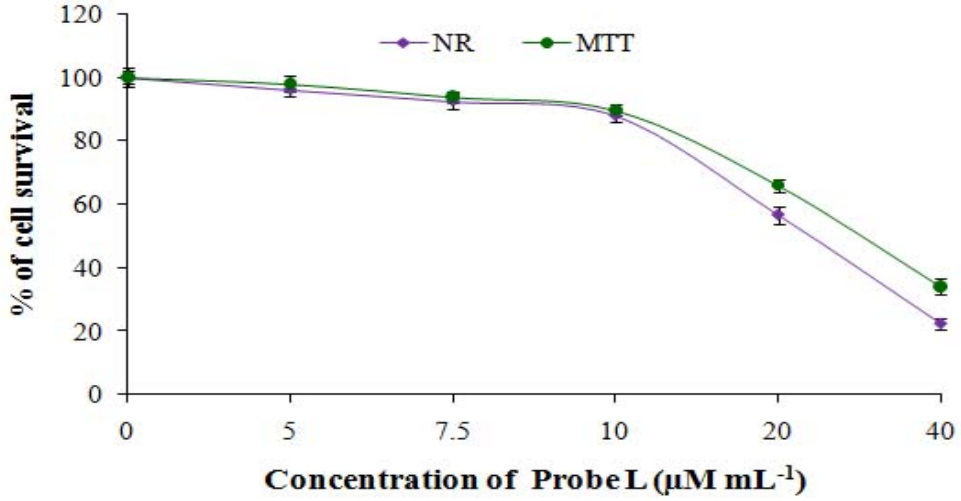


**Fig. 11S.** *In vitro* cytotoxicity of probe **L** to gill cell line of *Danio rerio* (*Dr*G) after 24 h exposure by MTT, NR uptake assay. The individual data points are expressed as the arithmetic mean percentage of control (mean ± SE) (n = 8 replicate)

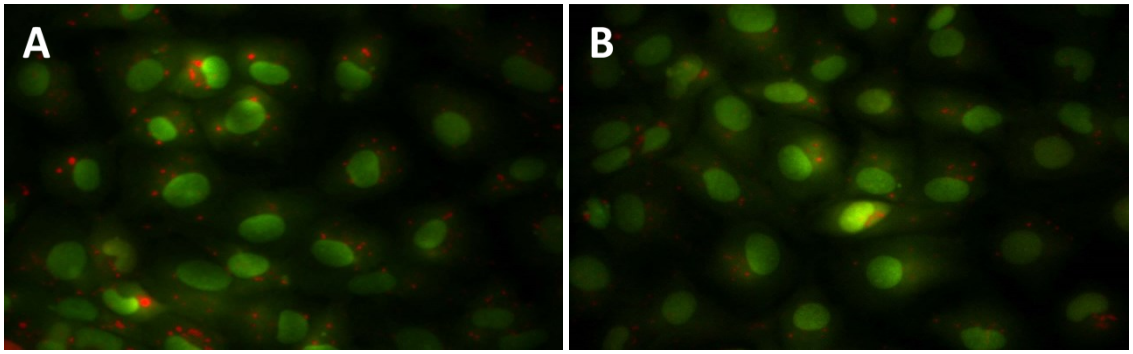


**Fig. 12S.** Fluorescence images of acridine orange and ethidium bromide staining. (**A**) *Dr*G cells exposed to Probe L (10 μM $mL^{-1}$) and (**B**) Control *Dr*G cells, images were captured at 400 × magnification.

**Table 1S.** Observed photophysical properties of Ligand **L** in different solvents

| **Solvent** | $\lambda_{Abs}$ (nm) | $\lambda_{Em}$ (nm) | **Stokes Shift** | | **Quantum Yield**[a] |
|---|---|---|---|---|---|
| | | | (nm) | ($cm^{-1}$) | |
| $CHCl_3$ | 439 | 468 | 29 | 1411 | 0.22 |
| ACN | 437 | 485 | 48 | 2265 | 0.05 |
| DMF | 436 | 495 | 59 | 2734 | 0.03 |
| DCM | 439 | 471 | 32 | 1548 | 0.09 |
| THF | 432 | 473 | 41 | 2007 | 0.11 |
| DMSO | 438 | 490 | 52 | 2423 | 0.09 |
| Toluene | 432 | 460 | 28 | 1409 | 0.12 |
| EtOAc | 430 | 469 | 39 | 1934 | 0.19 |
| MeOH | 454 | 491 | 37 | 1660 | 0.07 |
| EtOH | 436 | 481 | 45 | 2146 | 0.06 |

[a] Estimated by comparative William's method by using quinine sulfate as reference.

**Table 2S.** Fluorogenic performance of **L** towards $Lu^{3+}$ recognition and its comparison with previously reported work

| **Name of the Probe** | **$\lambda_{ext}$** (nm) | **$\lambda_{em}$** (nm) | **LOD** (nM) | **$K_a$** ($M^{-1}$) | **pH** | **Interference** | **Biological applications** |
|---|---|---|---|---|---|---|---|
| 8-hydroxyquinoline functionalized mesoporous silica[16] | 360 | 490 | 40 | $2 \times 10^6$ | 3.3 to 8.3 | $Al^{3+}$, $Tb^{3+}$, $Nd^{3+}$ | NS |
| 8-hydroxyquinoline functionalized mesoporous silica[17] | 310 | 486 | 82 | $5 \times 10^6$ | 3.3 to 8.3 | $La^{3+}$, $Pr^{3+}$ | NS |
| N-[3-methyl]-2-[pyridine-2-amido] phenyl] pyridine-2-carboxamide[18] | 310 | 462 | 860 | $2 \times 10^6$ | NS | $Er^{3+}$, $Sm^{3+}$, $Fe^{3+}$ | NS |
| N-(3-methoxy-4-hydroxybenzylidene)salicyloylhydrazone[19] | 365 | 426 | 93.2 | $1.36 \times 10^4$ | NS | NS | *In vitro C*ell imaging |
| (3-((diphenylphosphoryl)(hydroxy) methyl)-6-methylquinolin-2(1H)-one)[15] | 280 | 394 | 24.2 | $5.1 \times 10^5$ | 3.0 to 9.0 | No interference | NS |
| L (Present work) | 461 | 504 | 23 | $1.43 \times 10^4$ | 2.0 to 5.0 | No interference | *In vitro* and *In vivo* studies using the zebrafish model |